RADIATION DAMAGE OF GALLIUM ARSENIDE PRODUCTION CELLS

N. Mardesich, D. Joslin, J. Garlick, D. Lillington, M. Gillanders, B. Cavicchi
Spectrolab, Inc.
Sylmar, California
and
J. Scott-Monck, R. Kachare, and B. Anspaugh
Jet Propulsion Laboratory
Pasadena, California

In 1985 a process for manufacturing gallium arsenide solar cells by Liquid Phase Epitaxy (LPE) was transferred from Hughes Research Laboratories, Malibu to Spectrolab, Inc. The process, involving the growth of GaAs and AlGaAs from a super cooled liquid gallium semi-infinite melt has been described elsewhere (Reference 1) and will not be repeated here. Existing facilities allow the fabrication of up to 15,000, 2 cm x 4 cm (or equivalent area) GaAs cells of 17% nominal efficiency with the provision for rapid scale-up when required.

In a joint study with Jet Propulsion Laboratory (JPL) we have irradiated high efficiency LPE GaAs cells made on our manufacturing line with 1 MeV electrons up to fluences of $1x10^{16}$ cm^{-2}. Measurements of spectral response and dark and illuminated I-V data were made at each fluence and then, using computer codes developed here for our HP3000 "in-house" computer, we have fitted experimental data to our GaAs cell models. In this way it has been possible to determine the extent of the damage, and hence damage coefficients in both the emitter and base of the cell.

CELL DESCRIPTION

Cells manufactured for this test were produced on Spectrolab's GaAs LPE production line. The cross-sectional view of the device is illustrated in Figure 1, where a nominal 300 μm substrate was used to produce a 7 μm buffer, 0.45 μm emitter and 0.40 μm window. The typical dopant concentrations in the substrate, buffer and emitter were $2x10^{18}$ Si/cc, $2x10^{17}$ Sn/cc and $2x10^{18}$ Be/cc respectively. The ohmic contacts were made directly to the P- GaAs and N+ GaAs (substrate) for the front and back respectively.

Typical production cells of 16.7% (AM0) average efficiency, (22.6 mW/cm^2), were used in the radiation evaluation. I_{sc} and V_{oc} were nominally 28.7 mA/cm and 985 mV respectively.

With the limited number of pilot runs which have been produced, the typical electrical yield of devices above 16.0% (average above 16.5%) was 75%. Figure 2 is a composite graph of 5 lots manufactured over the period from July through September.

THEORETICAL BASIS FOR ANALYSIS

Computer models have been developed by Spectrolab for windowed gallium arsenide cells (Reference 2). These can provide from basic cell parameters (see Table 1) such as diffusion lengths for carriers in the various cell layers, a prediction of cell performance. These outputs give overall parameters such as I_{sc}, V_{oc}, P_{max}, CFF, etc., as well as spectral response for cells, as functions of radiation damage. The models

give the component spectral response due to window, emitter, junction and buffer as well as the overall spectral response. A typical output is shown in Figure 3 for BOL and for EOL (ϕ = 1E16 e/cm^2). An important feature of the spectral analysis is that at a wavelength of .5 μm the response is almost entirely due to the emitter. This makes it possible to deduce the emitter damage coefficient separately from that in the buffer. Then since the analysis gives the component ratios for the long wavelength response (.88 μm) the .5 μm data can be used to find the emitter component at .88 μm and hence to determine the buffer damage coefficient.

The modeling (as discussed in Reference 2) examines the effect of first diode (diffusion limited behavior) and of the second diode (depletion layer recombination limited behavior). The latter is important in high band gap cells such as gallium arsenide. In addition to the obvious parameters I_{sc}, V_{oc}, etc., the model analysis also gives the saturation currents for the first and second diodes (I_{01} and I_{02} respectively) as functions of the radiation damage.

TEST EQUIPMENT AND SET-UP

The current-voltage (I-V) characteristic, as recorded for cells before and after irradiation, was accomplished with the aid of a computerized data acquisition system. The system acquires 300 data points, which are stored into memory and then manipulated to produce the I-V curve, short circuit current (I_{sc}), open circuit voltage (V_{oc}), and maximum power operating point (P_{max}).

The simulator used in this test is designated Spectrolab X-25. It's AMO intensity was set using a GaAs encapsulated secondary standard 83-156 traceable to balloon flown standard 80-132. However, unirradiated sister cells to the ones tested were measured before and after irradiation to verify simulator intensity. Irradiated balloon flown standard 85-132 was also used to verify correct blue-red color ratio. The sample temperature on the test block was held to 28 $\pm$ 1°C by water cooling the block.

The instrumentation used to measure the spectral irradiance of the simulator was an Optronics Spectroradiometer with a Hewlett Packard 85 computer used for converting detector current to irradiance values, and for system control. The lower and upper limits of the range was 280 nm and 1050 nm, respectively. The slit width on the monochrometer and the wavelength interval was 5 nm during both the calibration and the actual scan.

Spectrolab has developed a computerized data acquisition system for dark I-V measurement. The system based on a 10 bit D/A and A/D interface is driven by an Apple IIe computer and enables rapid I-V measurement to be made over six orders of magnitude of current. Algorithms within the computer code allow the determination I_{01}, I_{02} and shunt resistance to be made and also a hard copy may be made on an HP X-Y recorder. The system is bipolar, enabling forward and reverse measurements to be made with ease.

Spectral response measurements were made by use of a computer controlled multifilter system. Twenty optical filters cover the expected cell response range with "crowding" filters at crucial parts of the spectrum for gallium arsenide cells (.4 - .5 and .8 to .9 μm respectively). At each filter position many readings are taken and averaged to increase accuracy and the system is calibrated by a sub-standard silicon cell with a spectral range much greater than that of gallium arsenide. This cell was calibrated against a silicon diode calibrated at Optoelectronics Laboratories

and also had formed one of a group of cells circulated among various establishments by Spectrolab in an attempt to standardize interlaboratory results. The system output gives cell response in mA/mW and also the quantum efficiency at each wavelength. An integration procedure gives an estimate of I_{sc} at AMO from the spectral data and this can be compared with I_{sc} data from the AMO simulator.

RESULTS

The cells used for irradiation were divided into four groups. The first group were held as standards and were not irradiated. The second group were irradiated to 10^{14}, $9X10^{14}$, $2.0x10^{15}$ and $7x10^{15}$ e^-/cm^2. The cells were tested at every level and a few cells were held as controls at each level. The third group were irradiated to $9X10^{14}$, $2.0x10^{15}$ and $7x10^{15}$ e^-/cm^2 for a total dosage of $9.9x10^{15}/cm^2$. Cells at each dosage level were also held as controls. The fourth and final group were irradiated to $7x10^{15}$ e/cm^2. The average P/P_o, J_{sc}/J_{sco} or V_{oc}/V_{oco} of the total starting group were within $\pm$ 0.3% of the final diminished group receiving the total dosage.

Table 2 and Figure 4 represent the degradation of the average cell and typical I-V curve for cells in group 2. This data is plotted in Figure 5 as a function of fluence. Representative spectral response curves for the range of fluence are plotted in Figure 6. Table 2 includes predicted values (in brackets) from the cell model using the parameters of Table 1.

From the response spectra of cells under the various fluences the variation at certain chosen wavelengths was determined. The results are plotted in Figure 7 for the wavelengths of .5 μm and .88 μm together with the overall I_{sc} calculated from the full spectral response. Also included is the plot for I_{sc} taken from the X-25 simulator measurements. These curves now have to be compared with those deduced from the modeling. The main cell specifications are as in Table 1 but parameters such as damage coefficients are varied to test fits with data. The broken curves in Figure 7 give the modeling curves for emitter and buffer damage coefficients of $3.5.10^{-8}$ and 2.10^{-7}/e respectively. A discussion of the comparative behavior is given below.

DISCUSSION

As shown by Table 2 the results of the 1 MeV electron irradiation tests can be predicted by the model using appropriate damage coefficients for emitter and buffer. We have chosen first to match these to prediction of I_{sc} values which depend on the total surface interface velocity between emitter and window. The model V_{oc} values at BOL are then too large but this is likely to be due to the fact that under the front grid contacts which penetrate into the emitter much higher velocities occur. Computation then shows that under V_{oc} conditions the experimental BOL value of V_{oc} would be obtained if the velocity averages 2.10^6 cm/s indicating much higher values under the contacts.

From dark state current-voltage curves we have computed the second diode (depletion layer recombination) saturation currents (I_{02}) as functions of damage. Initially, for the model parameters of Table 1 the value of I_{02} is about $5\text{-}6.10^{-11}$ A/cm^2 and at EOL (10^{16} e/cm^2) it is about $8\text{-}9.10^{-10}$ A/cm^2 i.e. a factor of 7 higher. The model gives a BOL value of 5.10^{-11} A/cm^2, close to the experimental value; at 10^{16} e/cm^2 fluence it is also about 7 times higher.

The extensive spectral response measurements in this work afford an opportunity to test the model. The data in Figure 7 at .5μm give the ability to see damage in

the emitter almost exclusively while the data at .88μm give the combined buffer, junction and emitter effects. In this region the discrepancies between model and experiment are evident. To match the .88μm values the damage coefficient for emitter would have to be increased so much that the .5μm data would not correlate with the model. There is clearly a situation here which needs to be followed up by model review and by further, more detailed analysis of the spectral data.

In conclusion we have carried out extensive studies of the effects of 1 MeV electron damage in gallium arsenide windowed cells. Overall the results are very similar to those published earlier by Mitsubishi (Reference 3) and by Hughes Research Laboratories (Reference 4). This is very significant since these devices were manufactured by us and these companies at different times; only the LPE layer growth is similar. We have extended diagnostics to include dark current-voltage curves and to detailed spectral analysis. What has been revealed is that overall modeling is satisfactory but that there are significant and interesting discrepancies which demand further attention.

Reference 1 - Mardesich, N. IEEE Proc. 18th PVSC, P.105 (1985)

Reference 2 - Garlick, G.F.J. IEEE Proc. 18th PVSC, P.854 (1985)

Reference 3 - Kato, M. IEEE Proc. 18th PVSC, P.652 (1985)

Reference 4 - Anspaugh, B. et al. Solar Cell Radiation Handbook 3rd Ed. JPL Publication 82-69 1982

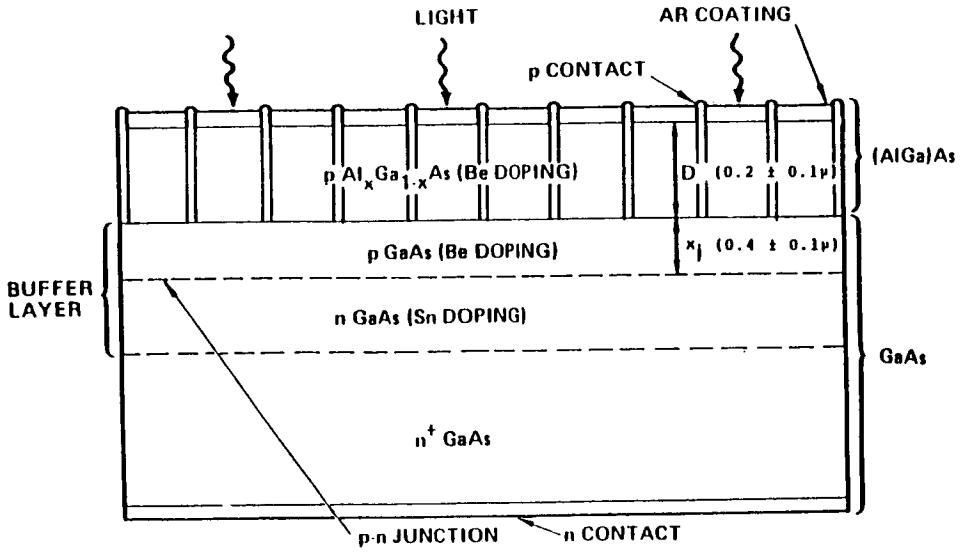

FIGURE 1. CROSS-SECTIONAL VIEW OF GaAs SOLAR CELL

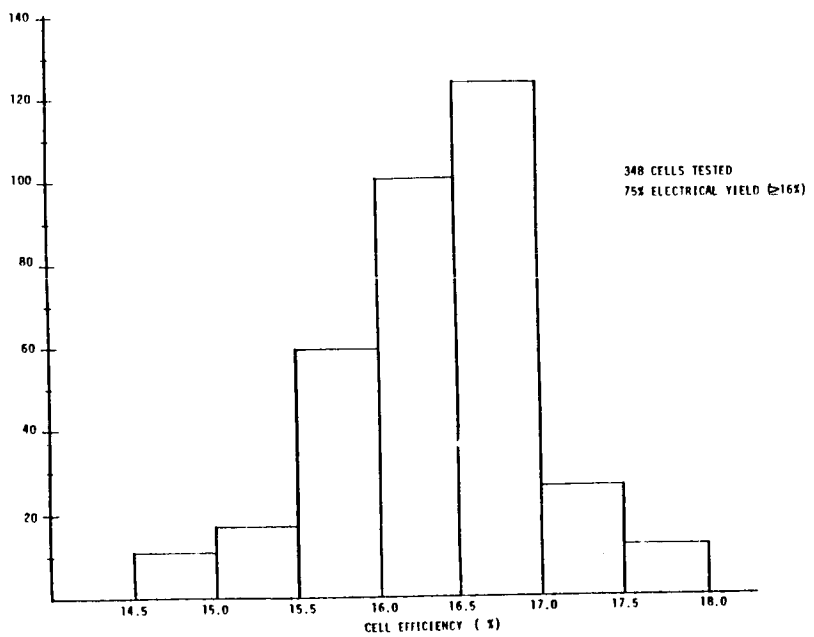

FIGURE 2. EFFICIENCY DISTRIBUTION OF GaAs CELL (4.30 CM^2)

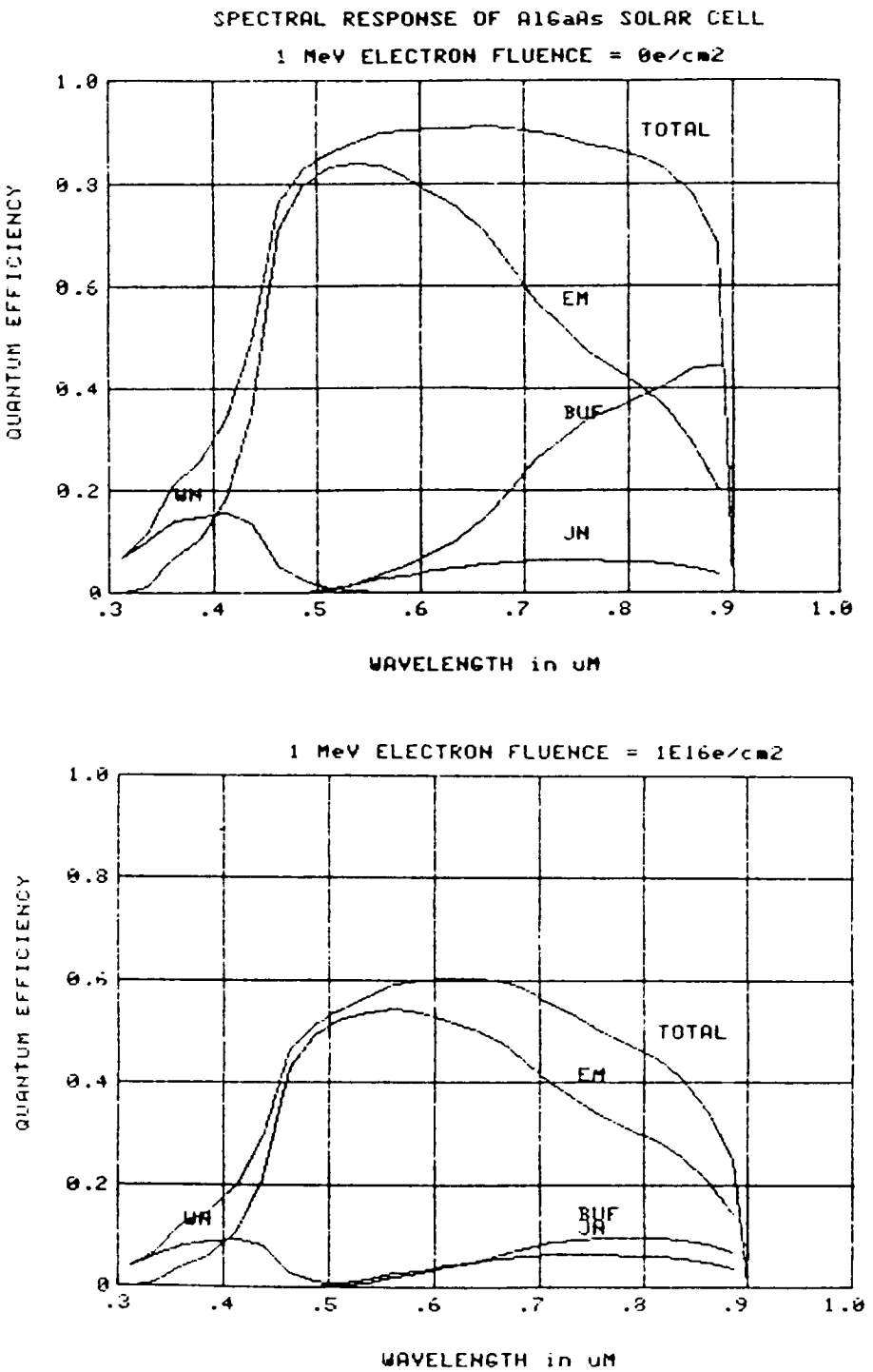

FIGURE 3. CALCULATED SPECTRAL RESPONSE OF GaAs CELL AT ZERO AND 10^{16} e-/cm^2 FLUENCE

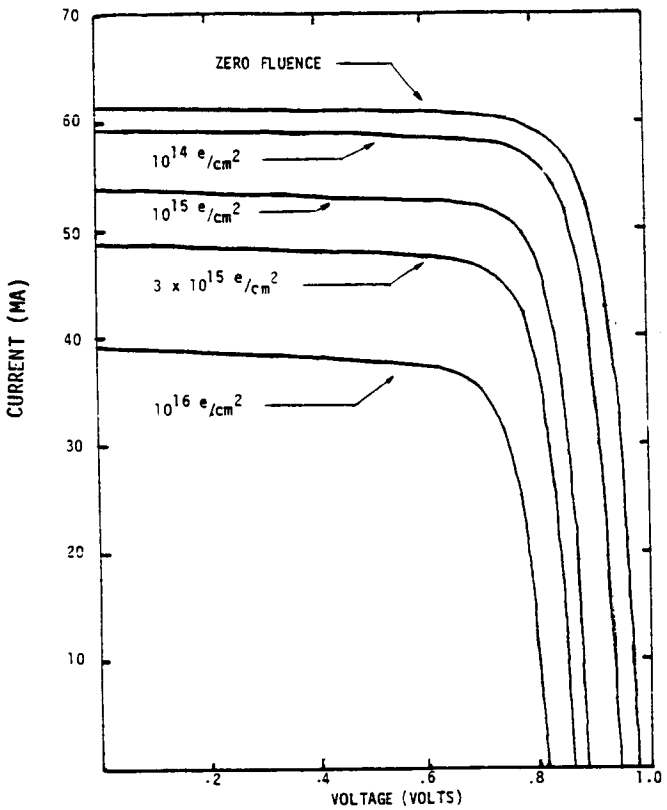

FIGURE 4. I-V CURVE OF A TYPICAL GaAs CELL AT VARYING 1 MeV FLUENCE

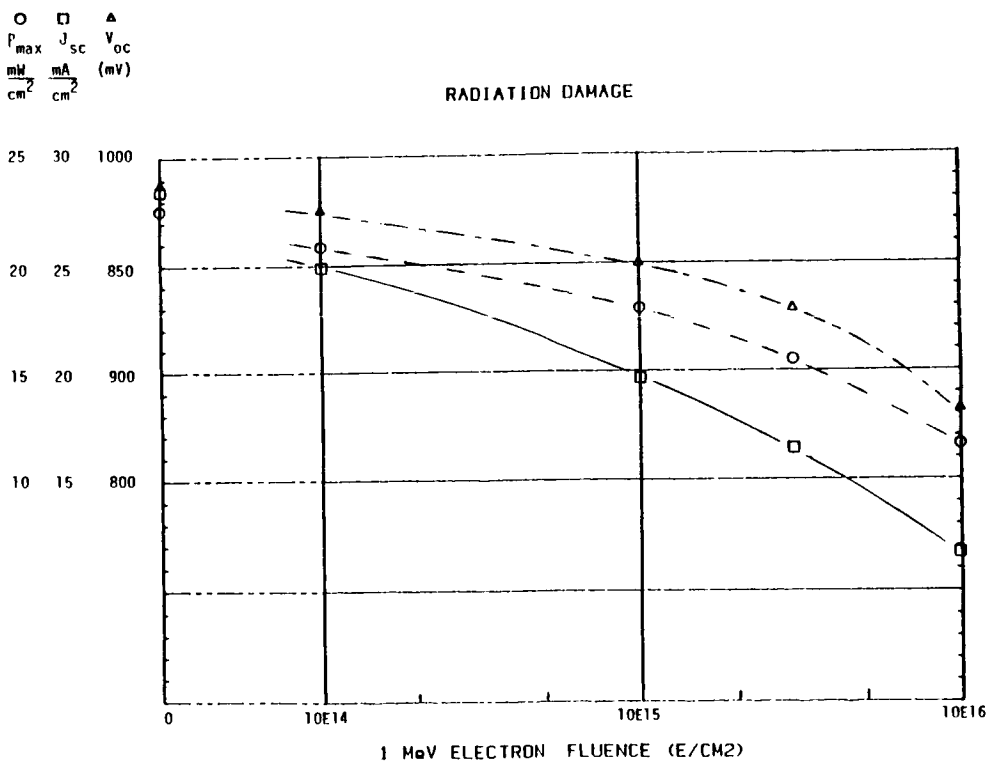

FIGURE 5. P_m, I_{sc}, AND V_{oc} vs. 1 MeV ELECTRON FLUENCE FOR TYPICAL GaAs CELL

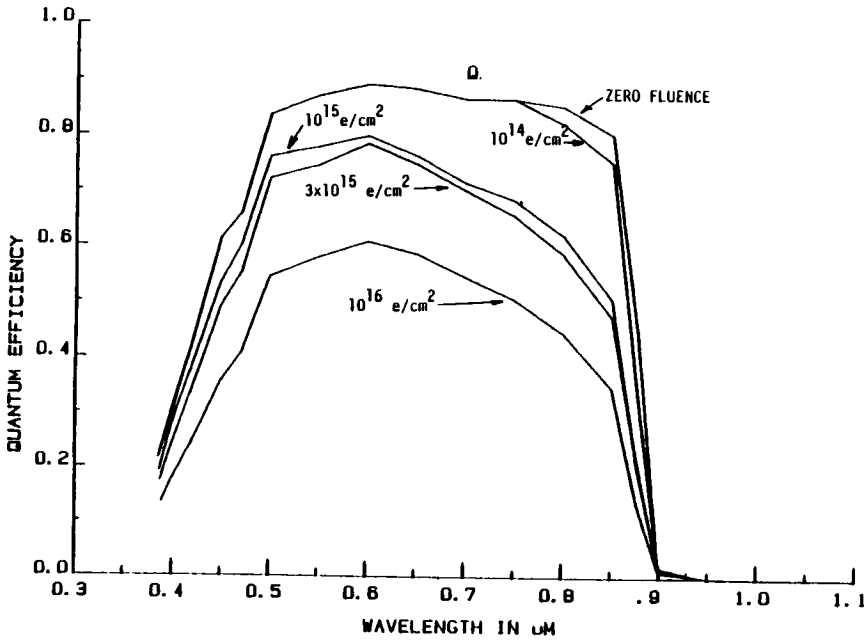

FIGURE 6: QUANTUM EFFICIENCY DEGRADATION AS A FUNCTION OF 1 MeV ELECTRONS

RADIATION DAMAGE

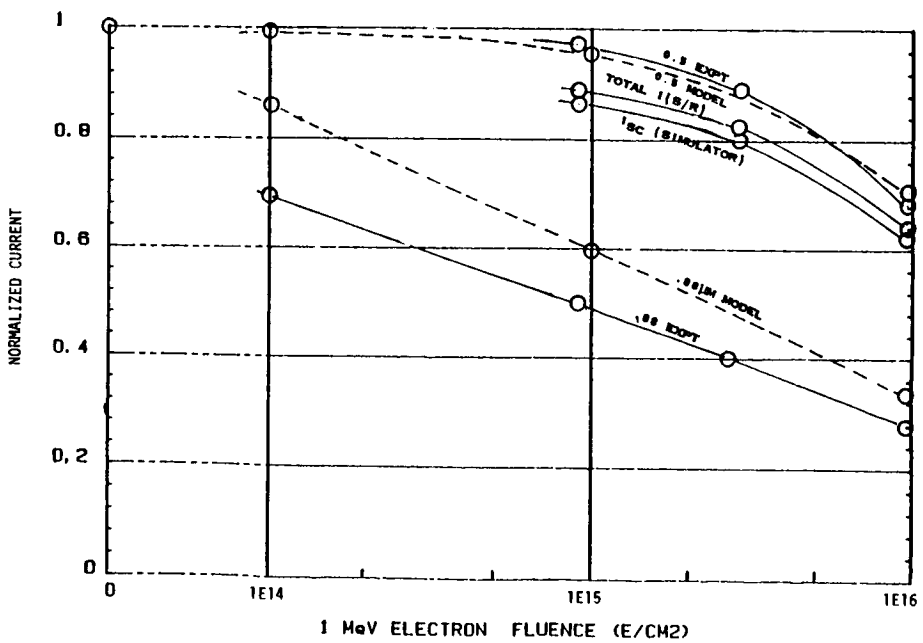

FIGURE 7: I_{SC} (AMO) I_{SC} (SPECTRAL RESPONSE), I_{SC} (.5μm) AND I_{SC} (.88μm) AS A FUNCTION OF 1 MeV ELECTRONS COMPARED TO THEORETICAL MODEL

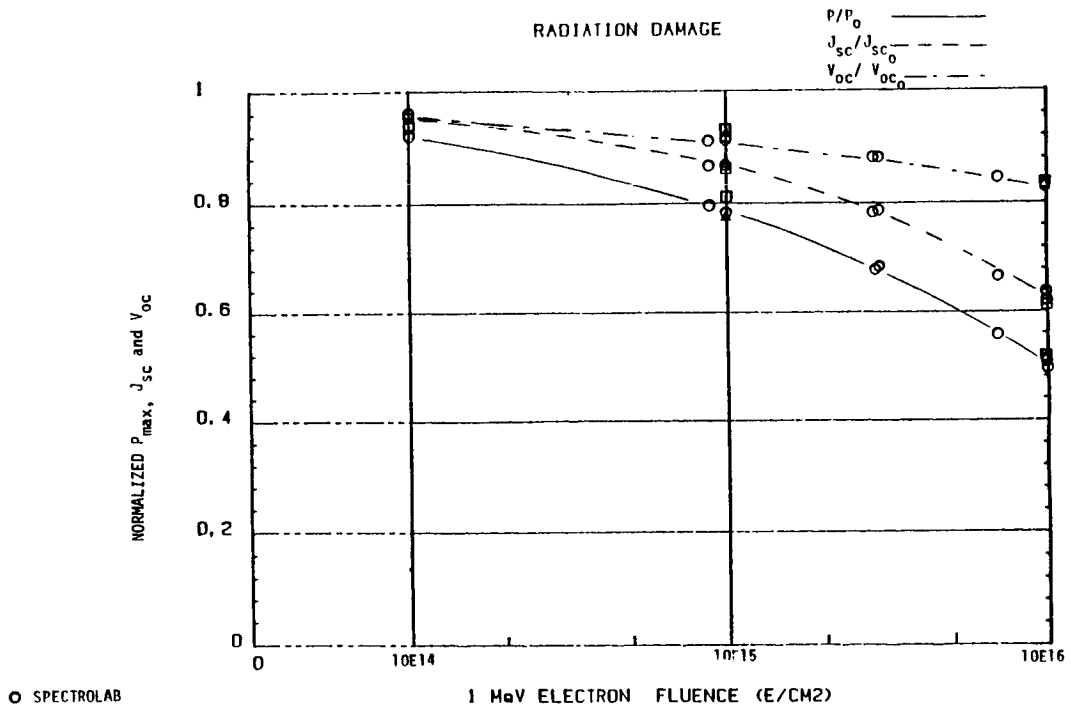

FIGURE 8. NORMALIZED P_{max}, I_{sc}, AND V_{oc} AS A FUNCTION OF 1 MeV ELECTRONS FOR RECENT TEST AND PUBLISHED DATA

TABLE 1

TYPICAL CELL PARAMETERS FOR MODELING OF CHARACTERISTICS TO MATCH EXPERIMENTAL DATA

WINDOW LAYER	
Thickness	.5 µm
Diffusion length	.2 µm
Diffusion coefficient	.27cm^2/s
Surface recombination velocity	10^6 cm/s
Doping concentration	2.10^{18}/cm^3
EMITTER LAYER	
Thickness	.5 µm
Diffusion length	5 µm
Diffusion coefficient	90cm^2/s
Interface recombination velcity	3.10^5 cm/s
Doping concentration	2.10^{18}/cm^3
BUFFER LAYER	
Thickness	7 µm
Diffusion length	2 µm
Diffusion coefficient	5 cm^2/s
Doping concentration	2.10^{17}/cm^3
DAMAGE COEFFICIENTS	
Emitter	$3.5.10^{-8}$/e
Buffer	$1.8.10^{-7}$/e

TABLE 2

FLUENCE (e/cm^2)	V_{oc} (mV)	I^{sc} (mA/cm^2)	P_{max} (mW/cm^2)	FF
0	984	28.7	22.6	.800
	(1006)	(28.0)	(22.8)	
10^{14}	948	27.5	20.9	.802
	(992)	(27.63)	(21.86)	
10^{15}	896	25.0	17.9	.800
	(933)	(25.77)	(18.5)	
3×10^{15}	863	22.7	15.4	.788
10^{16}	817	18.3	11.5	.769
	(812)	(18.14)	(11.09)	

*Bracketed values are model predictions

AVERAGE V_{oc}, J_{sc}, P_{max}, FF OF GROUP 2 GaAs SOLAR CELLS AFTER 1 MeV FLUENCE

N87-26438

PERFORMANCE OF AlGaAs, GaAs, AND InGaAs CELLS AFTER 1 MeV ELECTRON IRRADIATION

Henry B. Curtis and Russell E. Hart Jr.
NASA Lewis Research Center
Cleveland, Ohio

Electron irradiations (1 MeV) were made on three different types of III-V cells. AlGaAs, GaAs, and InGaAs cells with bandgaps of approximately 1.72, 1.43, and 1.1 eV, respectively, were tested. All of the cells were concentrator cells and performance data from 1 sun to beyond 100x AM0 were taken. The total 1 MeV electron fluence was $3x10^{15}$ e/cm^2 with data taken at several intermediate fluences. Cell performance is presented as a function of electron fluence for various concentration ratios and two different temperatures (25 and 80 °C). Since these three cell types are potential candidates for the individual cells in a cascade structure, it is possible to calculate the loss in performance of cascade cells under 1 MeV electron irradiation. Data are presented which show the calculated performance of both series-connected and separately connected cascade cells.

INTRODUCTION

For many years concentrator photovoltaic (PV) systems have been under strong consideration for use in space. The advantages of concentrator PV include higher cell efficiency, better radiation resistance, and a cost effective way of using advanced PV technology such as multijunction cells. Several optical designs are being studied such as the minature Cassegrainian system developed by TRW (ref. 1) and the SLATS trough system developed by General Dynamics. Both designs utilize small cells with illuminated areas that are a fraction of a square centimeter.

One of the concerns about concentrator PV is the effect of particle radiation on the cell performance at concentrated light levels. As part of an ongoing program at NASA Lewis Research Center, we have irradiated several types of concentrator cells with 1 MeV electrons and measured the performance degradation. Results for several GaAs cells were presented at the 18th IEEE Photovoltaic Specialists Conference (PVSC)(ref. 2). The results presented here are for AlGaAs, GaAs, and InGaAs cells irradiated with 1 MeV electrons to a fluence of $3x10^{15}$ e/cm^2. Results are also given for the calculated performance of multijunction cells under 1 MeV electron irradiation.

CELL DESCRIPTION

All the cells used in these irradiations were made by Varian. The bandgaps were 1.72 eV for the AlGaAs cells, 1.43 eV for the GaAs cells, and 1.1 eV for the InGaAs cells. The cells are all OM-VPE grown with an appropriate AlGaAs window. The AlGaAs cells were n/p while the GaAs and InGaAs cells were p/n. The GaAs cells had a junction depth of 0.5 μm, and the AlGaAs and InGaAs were about the same. There were a minimum number of cells available for this effort and some care should be taken in analyzing the data. There were four GaAs cells irradiated along with

two each of the AlGaAs and InGaAs cells. A summary of cell bandgaps and illuminated diameters is given in table I.

EXPERIMENTAL DESCRIPTION

All small area concentrator cells were individually mounted in separate cell holders. For the GaAs and AlGaAs cells, the holders consisted of a small bottom metal base and a washer-like metal top with a beveled hole slightly larger than the illuminated area of the cell. These two pieces supplied both a permanent support for the cell and an area for the four-wire electrical attachment. There was no soldering or welding of any contact to any cell. The InGaAs cells were mounted in Varian holders with top contacts attached directly to the outer busbar. The cells remained in their holders throughout all electron irradiations and performance measurements. There were no cover glasses attached to the cells, nor was there any shielding by optical elements during the irradiations.

Electron irradiations using 1 MeV electrons were performed at the NASA Lewis dynamitron and at the Naval Research Laboratory (NRL) Van de Graff generator. The cells were irradiated to a total fluence of 3×10^{15} e/cm^2, with performance measurements made at several intermediate fluence levels. The performance measurements consisted of the following:

1) Current-Voltage (I-V) data at 25 °C and 1 AM0 using an X-25 xenon solar simulator and a reference cell.

2) I-V data at 25 °C at several concentrations up to 100x AM0 and above using a pulsed xenon solar simulator and the linear assumption between irradiance and short-circuit current.

3) Short-circuit current data at one fixed concentration at both 25 and 80 °C in order to set the current scale at the elevated temperature.

4) I-V data at 80 °C at several concentrations as in step 2.

During I-V measurements the cells in their holders are mounted to a temperature-controlled block. The concentration level on the cell is varied by changing the distance from the light source and by using a Fresnel lens. Since the duration of the light pulse from the flash simulator is just 2 msec, there is no heating effect from the concentrated light. The elapsed time at 80 °C was about 30 min for each cell. Several repeat measurements were made at 1 sun and 25 °C after the elevated temperature measurements, in order to determine if any annealing had taken place.

RESULTS AND DISUSSION

Table II shows the average starting electrical parameters (before electron irradiation) for the three different cell types. Data are presented for 100x concentration levels at both 25 °C and 80 °C, and at AM0 25 °C. At the 100x concentration level, the cells show excellent efficiencies with the GaAs cells averaging over 21 percent at 25 °C and 20 percent at 80 °C. At 1 sun, the efficiencies were somewhat low because of shunting effects, which are unseen at the normal operating concentration levels.

Tables III, IV, and V show the ratios of short-circuit current, open-circuit voltage, fill factor, and maximum power after irradiation to the unirradiated values for several fluence levels at three different measurement conditions. Table III shows data for 25 °C at 1 sun, while tables IV and V show data for 100x concentration at 25 °C and 80 °C respectively. The ratios for short-circuit current at 25 °C are the same for both solar irradiation levels because of the linear current-irradiance assumption. The tables indicate that the bulk of the degradation is in the current with much smaller degradation in voltage and fill factor.

Figure 1 shows plots of normalized maximum power as a function of 1 MeV electron irradiance for the three cell types at 25 °C and 100x AM0. The InGaAs cells show more degradation at the higher fluences than the AlGaAs or GaAs cells. It is difficult to draw conclusions from these curves because they are based on a small number of cells (two each of AlGaAs and InGaAs and four of GaAs). However there may be a trend of more radiation resistance with increasing bandgap. If so, this would be beneficial for multijunction cells where the higher bandgap cells produce more of the power. Figures 2, 3, and 4 show similar data for short-circuit current (I_{SC}), open-circuit voltage (V_{OC}), and fill factor respectively. These curves show the major drop in power is due to loss of current as the 1 MeV fluence level increases.

Figures 1 to 4 show data taken at 25 °C. Typical operating temperatures on concentrator cells in space will be dependent on orbit, concentration level, cell size, and concentrator design. During this investigation data were taken at 80 °C, which would be a typical operating temperature. Figure 5 shows normalized maximum power at 100x AM0 for the AlGaAs cells as a function of 1 MeV electron fluence for two temperatures, 25 °C and 80 °C. The difference between data at the two temperatures is not that large. From tables IV and V, the spread in degradation between 25 °C and 80 °C for GaAs cells is smaller than the AlGaAs spread in figure 5, while it is a little larger for the InGaAs cells.

All the data presented have been for individual cells and are actual measured data. Since we have data for cells of different bandgaps, we can calculate the performance of multijunction cells under 1 MeV electron irradiation. The AlGaAs/InGaAs pair is a good candidate for this calculation since the bandgaps, 1.72 eV and 1.1 eV, are near the ideal pair for optimum multijunction performance. When the AlGaAs and InGaAs cells are operating as a multijunction cell, the bottom cell (InGaAs) is filtered by the AlGaAs cell and has less sunlight incident upon it. Since the bandgaps are near optimum for a series-connected multijunction cell, we reduced the irradiance on the bottom cell until the currents matched at the unirradiated fluence level. With 100x concentration on the AlGaAs cell, we had about 56x on the InGaAs cell. Since data were taken at several concentration levels at 25 °C at each fluence, we can readily obtain data for the InGaAs cell at 56x for all fluence levels.

Figure 6 shows normalized maximum power for the top AlGaAs cell and the "filtered" bottom InGaAs cell as a function of 1 MeV electron fluence. The curves are normalized to 1 for the top cell. Note that although the two curves look parallel, there is a much greater percentage drop for the InGaAs bottom cell as fluence increases. Figure 7 is a similar curve showing short-circuit current for the AlGaAs top cell and the "filtered" InGaAs cell. For the current data, the two curves diverge a large amount while starting at the same value at zero fluence.

There are two cases of multijunction cells of interest. One is the separately connected or 4-terminal structure, and the second is the series-connected structure. In the separately connected case, the performance of the multijunction cell can be calculated just by adding the maximum powers of the individual cells shown on figure 6. The series connected structure requires adding actual I-V curves in series. In this case, if the currents are mismatched, the output power will be less than the simple sum of the individual cell powers.

The diode equation was used to obtain I-V curves for the series connected case. The light-generated current was set to the desired short-circuit current while the coefficients of the injection term and space-charge recombination term were varied to match V_{OC} and fill factor. A series resistance of less than .05 ohm-cm^2 was used. We were than able to calculate an entire I-V curve to match any set of parameters. In order to add I-V curves with different currents, a reverse characteristic is required. For this work we assumed the curves broke down between -2 and -3 V.

Figure 8 shows the calculated degradation in maximum power (Pmax) for both the series-connected and separately connected (four-terminal) multijunction cells under 1 MeV electron irradiance. The operating conditions are 25 °C and 100x AM0 incident on the top cell. We also show the individual curves for the top AlGaAs and the "filtered" bottom InGaAs cells. Note that for very low fluences, the difference between series and separate connections is quite small. However as the currents of the two cells diverge at higher fluence levels, the series connected case falls to a point where the multijunction cell delivers less power than a bare AlGaAs cell would. This is due to the limiting action of the large current mismatch between the two individual cells.

The results of figure 8 indicate that for high-radiation missions, it may be necessary to use the separately connected version of multijunction cells because of the problems created by current mismatch. For shorter missions in a low radiation orbit, the series connected version would perform just as well as the four-terminal case. It must be noted that this work is based on 1 MeV electron irradiations only on a small number of cells. Further work is required to more completely investigate the radiation performance of multijunction cells.

ACKNOWLEDGMENTS

The electron irradiation facilities at NRL were made available through the cooperation of Richard Statler and Robert Farr.

REFERENCES

1. Patterson, R.E.: Preliminary Concept of a 100-Kilowatt Miniaturized Cassegrainian Concentrator Solar Array. Space Photovoltaic Research and Technology 1983, NASA CP-2314, 1983, pp. 157-162.

2. Curtis, H.B.; and Swartz, C.K.: Performance of GaAs and Silicon Concentrator Cells Under 1 MeV Electron Irradiation. 18th IEEE Photovoltaic Specialists Conference, IEEE, 1985, pp. 356-361.

TABLE I. - DESCRIPTION OF CELLS

Cell type	Bandgap, eV	Diameter, mm
AlGaAs	1.72	6.3
GaAs	1.43	4.0
InGaAs	1.10	6.3

TABLE II. - INITIAL I-V DATA

	Short-circuit current/cm^2, A	Open-circuit voltage, V	Fill factor	Efficiency, percent
100x AMO, 25 °C				
AlGaAs	1.996	1.376	0.836	16.9
GaAs	3.174	1.143	.792	21.2
InGaAs	3.580	.859	.794	18.1
100x AMO, 80 °C				
AlGaAs	2.069	1.264	0.802	15.5
GaAs	3.309	1.059	.772	20.0
InGaAs	3.648	.774	.775	16.2
AMO, 25 °C				
AlGaAs	19.96×10^{-3}	1.200	0.772	13.7
GaAs	31.74	.898	.762	16.0
InGaAs	35.80	.613	.655	10.6

TABLE III. - RATIOS OF IRRADIATED TO INITIAL VALUES FOR SEVERAL 1 MeV ELECTRON FLUENCES AT 25 °C and 1X

Fluence level, e/cm^2	Short-circuit current I_{sc}	Open-circuit voltage V_{oc}	Fill factor	Power Maximum
AlGaAs				
$1x10^{13}$	1.002	0.998	1.005	1.007
$3x10^{13}$	.998	.999	1.008	1.007
$1x10^{14}$	.993	.997	1.003	.993
$3x10^{14}$	.968	.987	1.003	.959
$1x10^{15}$	.909	.938	.986	.868
$3x10^{15}$	.821	.938	.971	.747
GaAs				
$1x10^{13}$	0.989	1.002	1.000	0.991
$3x10^{13}$	.978	.994	1.009	.981
$1x10^{14}$	.965	.993	1.007	.965
$3x10^{14}$	.927	.977	1.011	.923
$1x10^{15}$	.875	.957	1.020	.860
$3x10^{15}$	.776	.928	1.036	.750
InGaAs				
$1x10^{13}$	0.974	1.006	0.995	0.976
$3x10^{13}$	.973	.999	.996	.969
$1x10^{14}$	.942	.989	.995	.929
$3x10^{14}$	.879	.980	.998	.860
$1x10^{15}$	.687	.929	.995	.637
$3x10^{15}$	.460	.857	.989	.393

TABLE IV. - RATIOS OF IRRADIATED TO INITIAL VALUES FOR SEVERAL 1 MeV ELECTRON FLUENCES AT 25 °C and 100x

Fluence level, e/cm^2	Short-circuit current I_{sc}	Open-circuit voltage V_{oc}	Fill factor	Power Maximum
AlGaAs				
$1x10^{13}$	1.002	0.987	0.990	0.979
$3x10^{13}$	.998	.988	.977	.966
$1x10^{14}$	.993	.983	.975	.953
$3x10^{14}$	.968	.979	.963	.913
$1x10^{15}$	.909	.963	.969	.849
$3x10^{15}$	.821	.948	.938	.730
GaAs				
$1x10^{13}$	.989	.991	1.010	.989
$3x10^{13}$	.978	.975	1.029	.978
$1x10^{14}$	.965	.954	1.030	.947
$3x10^{14}$	.927	.925	1.027	.881
$1x10^{15}$	.875	.893	1.033	.807
$3x10^{15}$	.776	.859	1.029	.687
InGaAs				
$1x10^{13}$	.974	.996	.995	.963
$3x10^{13}$	.973	.998	.997	.968
$1x10^{14}$	.942	.988	.997	.926
$3x10^{14}$	.879	.971	.994	.847
$1x10^{15}$	.687	.933	.975	.623
$3x10^{15}$	.460	.889	.953	.389

TABLE V. - RATIOS OF IRRADIATED TO INITIAL VALUES FOR SEVERAL 1 MeV ELECTRON FLUENCES AT 80 °C and 100x

Fluence level, e/cm^2	Short-circuit current I_{sc}	Open-circuit voltage V_{oc}	Fill factor	Power Maximum
AlGaAs				
$1x10^{13}$	1.004	0.992	0.991	0.991
$3x10^{13}$	.996	.994	.988	.982
$1x10^{14}$	.998	.990	.983	.972
$3x10^{14}$	.977	.983	.979	.943
$1x10^{15}$	.926	.967	.970	.871
$3x10^{15}$	.839	.943	.968	.767
GaAs				
$1x10^{13}$	.988	.992	.999	.980
$3x10^{13}$	.980	.971	1.015	.966
$1x10^{14}$	.965	.947	1.024	.939
$3x10^{14}$	.925	.916	1.036	.871
$1x10^{15}$	.872	.879	1.025	.786
$3x10^{15}$	.779	.840	1.020	.670
InGaAS				
$1x10^{13}$	.977	.999	.986	.963
$3x10^{13}$	.976	.998	.986	.963
$1x10^{14}$	.951	.995	.990	.939
$3x10^{14}$	.899	.981	.985	.870
$1x10^{15}$	.748	.922	.968	.666
$3x10^{15}$	.527	.884	.946	.441

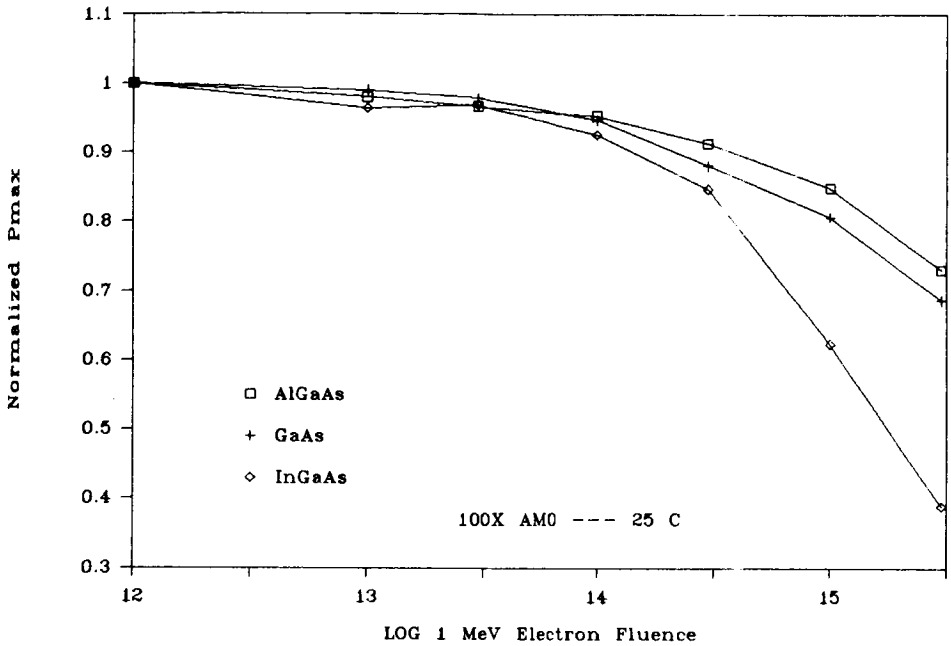

Figure 1. - Normalized maximum power for AlGaAs, GaAs, and InGaAs cells as function of 1 MeV electron fluence. (100x AM0, 25 °C)

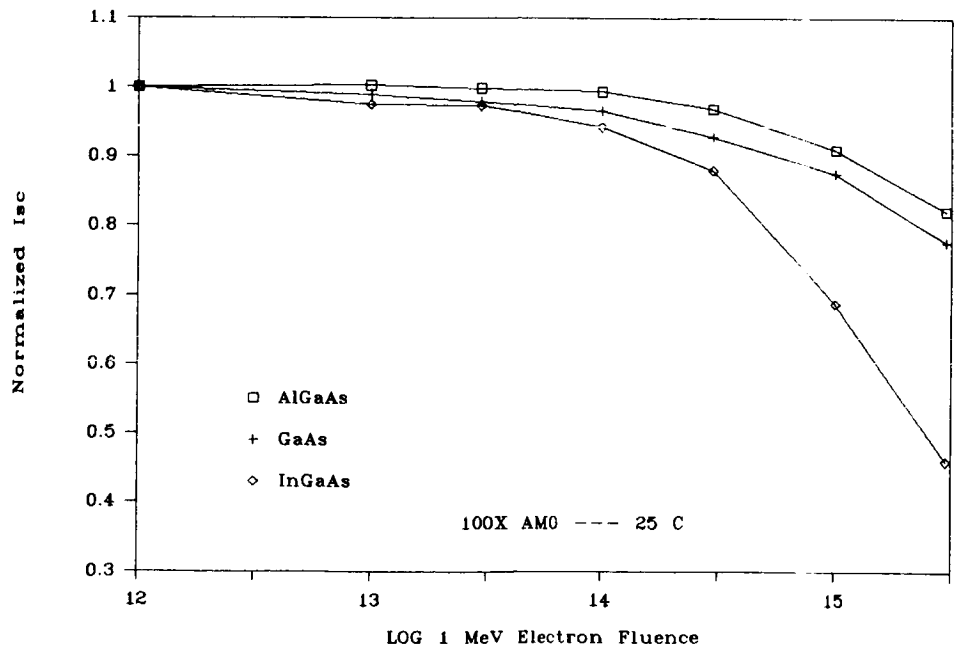

Figure 2. - Normalized short-circuit current for AlGaAs, GaAs, and InGaAs cells as function of 1 MeV electron fluence. (100x AM0, 25 °C)

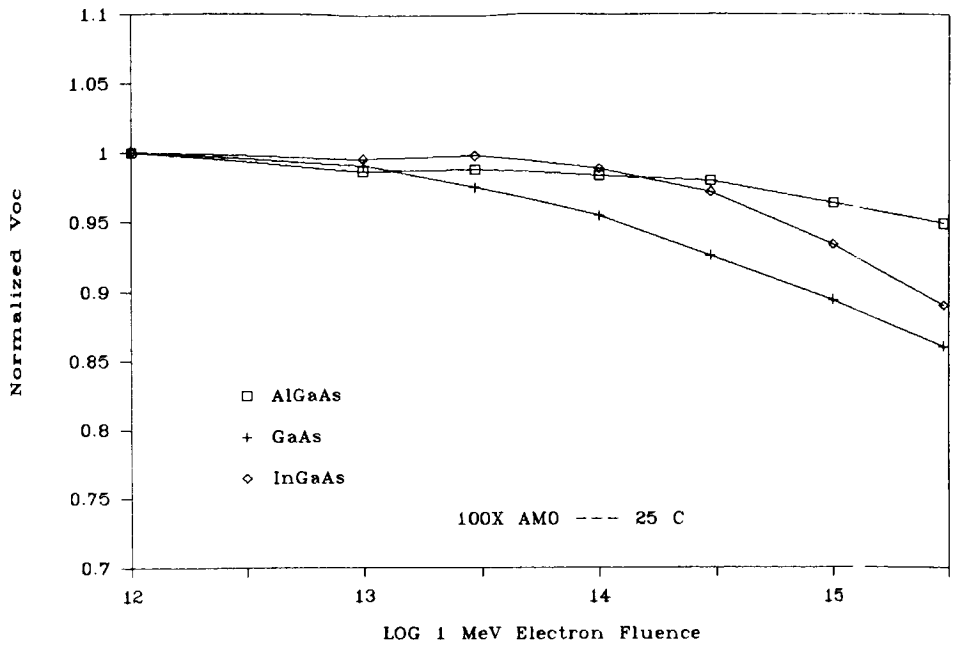

Figure 3. - Normalized open-circuit voltage for AlGaAs, GaAs, and InGaAs cells as function of 1 MeV electron fluence. (100x AMO, 25 °C)

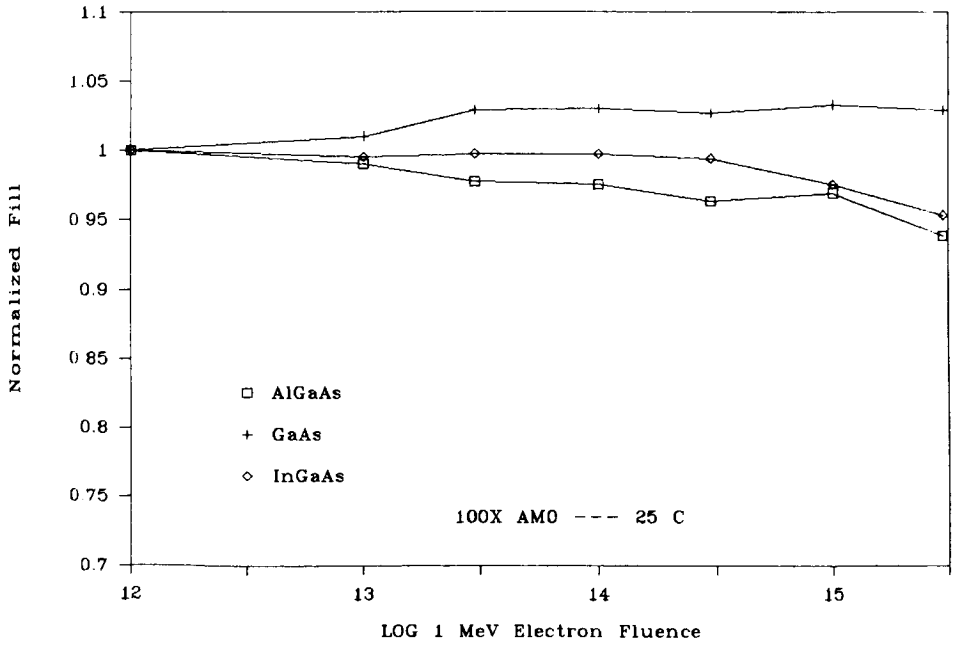

Figure 4. - Normalized fill factor for AlGaAs, GaAs, and InGaAs cells as function of 1 MeV electron fluence. (100x AMO, 25 °C)

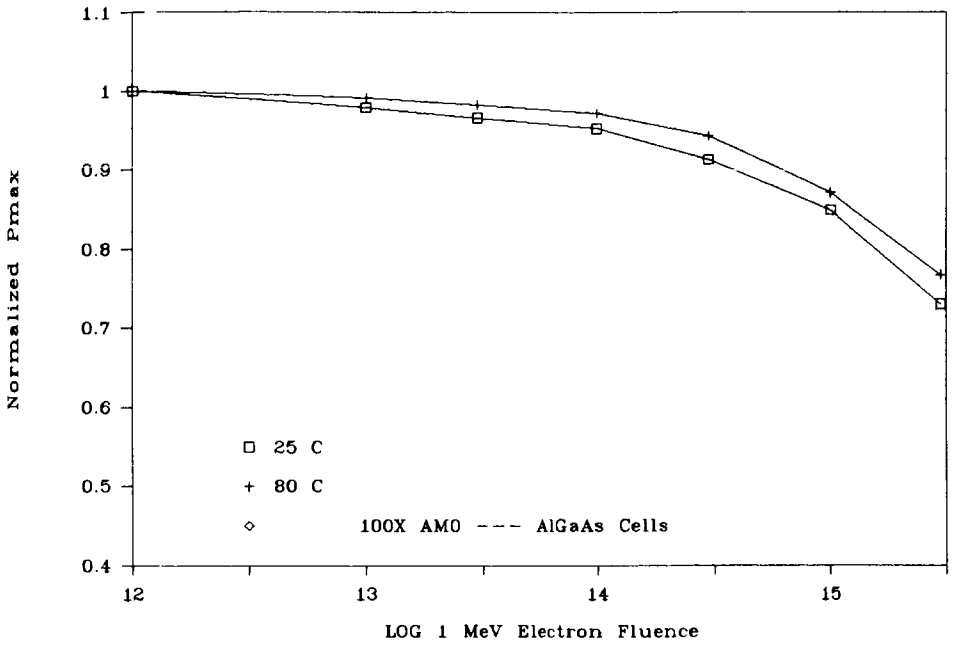

Figure 5. - Normalized maximum power for AlGaAs cells at 25 °C and 80 °C as function of 1 MeV electron fluence.

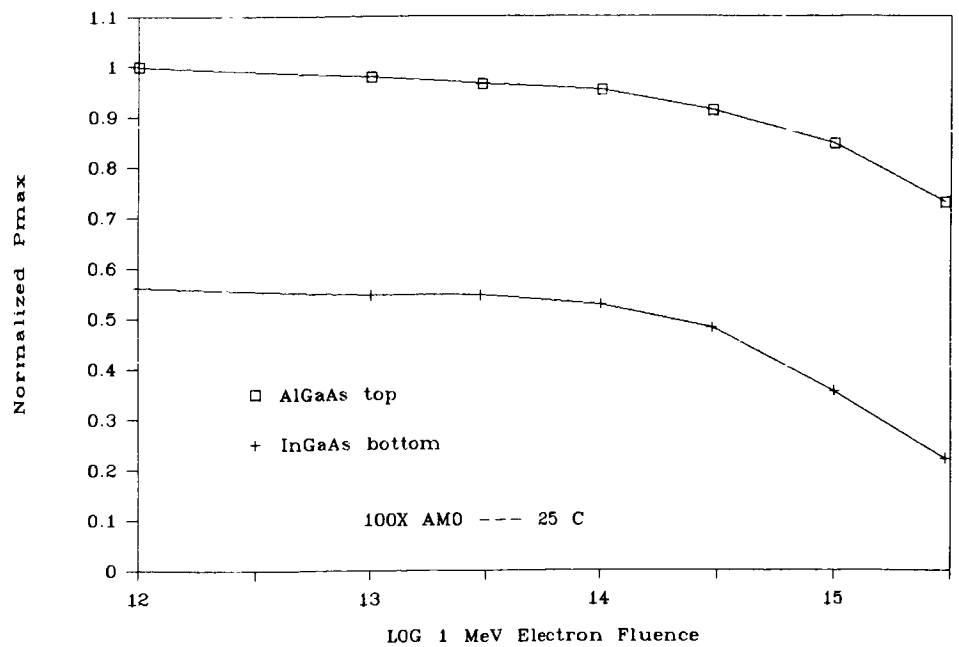

Figure 6. - Normalized maximum power for AlGaAs top cell and an InGaAs bottom cell at 25 °C with 100x AMO incident on top cell as function of 1 MeV electron fluence.

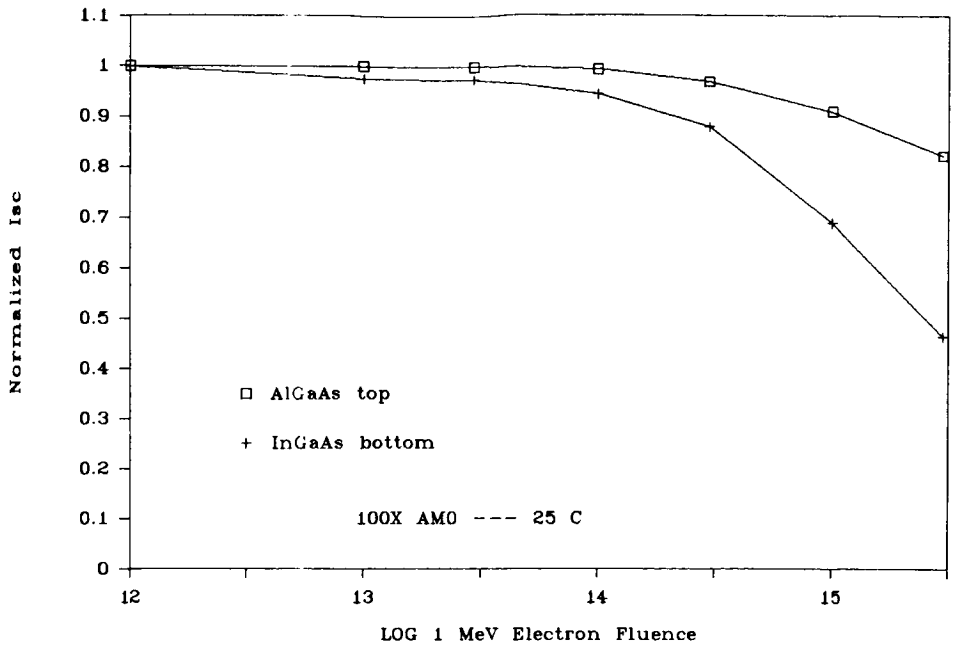

Figure 7. - Normalized short-circuit current for an AlGaAs top cell and an InGaAs bottom cell at 25 °C with 100x AM0 incident on top cell as function of 1 MeV electron fluence.

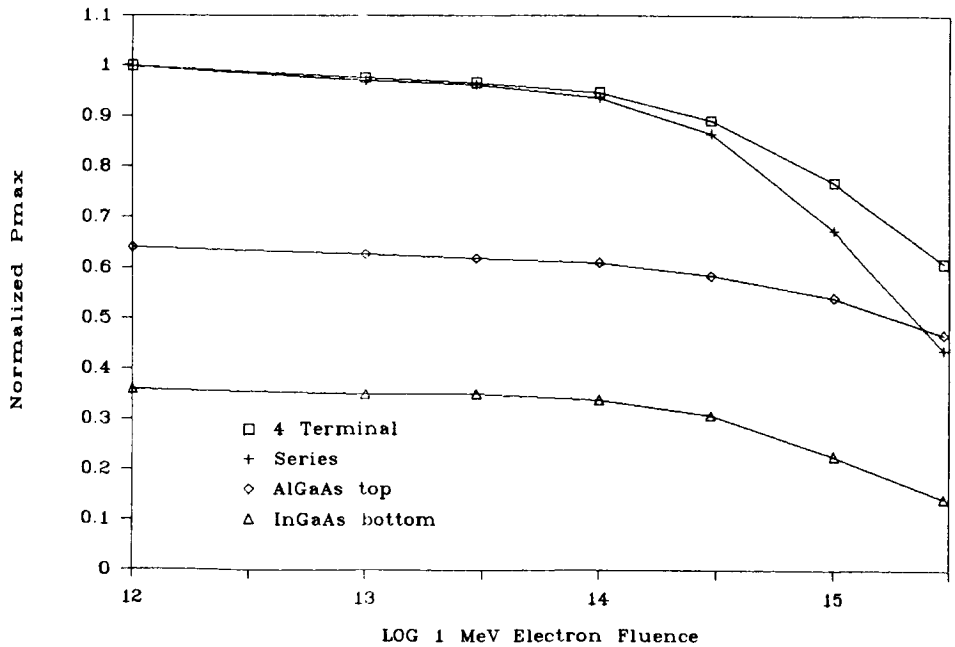

Figure 8. - Normalized maximum power for an AlGaAs/InGaAs cascade cell (series and separately connected) at 25 °C and 100x AM0 as function of 1 MeV electron fluence.